Int J Clin Exp Pathol 2014;7(4):1580-1587
www.ijcep.com /ISSN:1936-2625/IJCEP1402009

Original Article

Hyperlipidemia compromises homing efficiency of systemically transplanted BMSCs and inhibits bone regeneration

Quan-Chen Xu[1,2,3*], Peng-Jie Hao[4*], Xin-Bo Yu[2], Shu-Lan Chen[5], Mei-Jiao Yu[3,6], Jin Zhang[3,6], Pi-Shan Yang[1,3]

[1]Department of Periodontology, School of Dentistry, Shandong University, Jinan, China; [2]The Affiliated Hospital of Qingdao University Medical College, Qingdao, China; [3]Shandong Provincial Key Laboratory of Oral Biomedicine, Shandong University, Jinan, China; [4]Yantai Stomatological Hospital, Yantai, China; [5]Qingdao Municipal Hospital, Qingdao, China; [6]Department of Endodontics, School of Dentistry, Shandong University, Jinan, China. [*]Equal contributors.

Received February 3, 2014; Accepted March 10, 2014; Epub March 15, 2014; Published April 1, 2014

Abstract: Purpose: Mesenchymal stem cells (MSCs) can selectively home to bone defects and play an essential role in promoting bone regeneration. As an adverse effect factor for bone metabolism, hyperlipidemia significantly impairs bone regeneration. In this study, bone marrow stromal cells (BMSCs) were systemically transplanted into a hyperlipidemic mouse model to explore the effect of hyperlipidemia on stem cell recruitment and bone regeneration. Methods: Hyperlipidemia was established in ApoE$^{-/-}$ mice (on C57BL/6J background) fed with a high fat diet (HFD) for five weeks. C57BL/6 mice fed with the same diet served as controls. BMSCs labeled with the green fluorescent protein (GFP) were then injected via the tail vein and bone defects were created in the mandibles. The animals were sacrificed at weeks 1, 2 and 4 after surgery, and the fate of the transplanted BMSCs was monitored with a fluorescence microscope and immunohistochemical analysis. After hematoxylin and eosin (HE) staining and Masson's Trichrome (MT) staining, histomorphometric analysis was performed to evaluate bone regeneration. Results: In both groups transplanted with BMSCs, the number of GFP-positive BMSCs detected in the bone defects reached its peak at 1 week after surgery and was decreased thereafter. However, at all time points, less GFP^{+} cells were detected in the ApoE$^{-/-}$ mice than in the corresponding control mice. BMSCs transplantation significantly enhanced new bone formation, but to a lesser degree in the ApoE$^{-/-}$ mice when compared with the control mice. Conclusions: Hyperlipidemia compromises homing efficiency of systemically transplanted BMSCs and inhibits bone regeneration.

Keywords: Hyperlipidemia, homing efficiency, bone regeneration, mesenchymal stem cells, mice

Introduction

Bone defects in the oral and maxillofacial region usually interfere with normal masticatory function and often have devastating esthetic, emotional and social impact on patients. Physiological and functional reconstruction of the damaged tissues is highly expected, which requires not only the differentiation of local reparative cells but also the recruitment of mesenchymal stem cells (MSCs) from bone marrow and peripheral circulation [1-3]. In response to the injury stimuli, a series of cellular and molecular events are activated, various cytokines and growth factors are released by platelets and inflammatory cells, and eventually the MSCs are induced to migrate into the wound site. Recruited MSCs then proliferate and differentiate into osteoblasts, which actively participate in bone regeneration [1, 4].

Bone marrow stromal cells (BMSCs) are a type of pluripotent mesenchymal stem cells with the capacity for multipotent differentiation into tissues of mesodermal origin such as fat, bone, cartilage, ligament and more [5]. As the progenitor cells for osteoblasts, BMSCs have always played a substantial role in reconstitution of bone tissue [6, 7]. After systemic transplantation into irradiated mice with mandibular bone defects, BMSCs can be detected in the wound sites, undergo osteogenic differentiation and significantly promote local bone regeneration [8]. Although the mechanisms responsible for

the recruitment of BMSCs have not yet been fully revealed, accumulating lines of evidence suggest that cytokines and chemokines probably play critical roles in the mobilization of BMSCs and their subsequent homing to the injured tissues [9, 10]. However, currently it is still unclear whether systemic health conditions directly affect the homing efficiency of BMSCs.

An association between hyperlipidemia and osteoporosis has been suggested by a variety of studies. Epidemiologic evidence indicates the elevated serum lipid level as a risk factor of osteoporosis [11-13]. Furthermore, diet-induced hyperlipidemia leads to significantly reduction in bone mineral density (BMD) and bone mineral content (BMC) in animal models [14, 15], and lipid-lowering treatments increase BMD and lower fracture risk in humans [16, 17]. When treated with the oxidation products of low density lipoprotein (LDL) *in vitro*, BMSCs isolated from hyperlipidemic individuals underwent an adipogenic differentiation instead of osteogenic differentiation [18]. A recent study demonstrated hyperlipidemia impaired bone regeneration through actions of oxidized lipids [19]. Unfortunately, little is known whether hyperlipidemia disturbs the recruitment of BMSCs to the bone defect sites from peripheral circulation and further inhibits bone regeneration. In this study, hyperlipidemia was established using an ApoE deficient ($ApoE^{-/-}$) mouse model. Mandibular bone defects were then created in these mice and BMSCs labeled with the green fluorescent protein (GFP) were transplanted via the tail vein. The homing efficiency of transplanted BMSCs was evaluated and the new bone formation was determined using histomorphometric analysis.

Materials and methods

Animals and diet

Eight-week-old male $ApoE^{-/-}$ mice on C57BL/6J background and C57BL/6J mice (Peking University Health Science Center, Beijing, China) were fed on a high-fat/high-cholesterol/cholate diet (15%/1.25%/0.5%, respectively). Body weight of these animals was recorded every week. Fasting blood samples were taken from the angular vein of 8-wk-old and 12-wk-old animals to determine serum lipid levels including LDL, high density lipoprotein (HDL), triglyceride (TG) and total cholesterol (TC) using an autoanalyzer (Hitachi, Japan). This study was conducted in conformity with the Animal Care and Use Committee of Shandong University (Jinan, Shandong Province, China).

Isolation, culture and characterization of BMSCs

BMSCs were isolated from C57BL/6J mice (6-8 weeks old) and cultured as described previously [20]. BMSCs (1×10^6) at passage 4 were incubated with antibodies against mouse CD34, CD44, CD45 (BioLegend, USA) and CD29 (eBioscience, USA) for flow cytometry analysis with the use of CXP Analysis 2.1 software (Beckman Coulter, USA). To directly track the migration and differentiation of BMSCs *in vivo*, the BMSCs were labeled with a lentiviral vector encoding enhanced GFP (Cyagen, China). Briefly, the fourth-passage BMSCs (5×10^3 cells/cm^2) were incubated in 6-well plates for 24 h. Then the culture medium was removed and concentrated viral supernatant diluted in serum-free α-MEM was added. Eight hours later, the viral supernatant was replaced with complete culture medium. G418 (100 μg/ml) was used to purify the GFP-positive cells.

Animal surgery and BMSC transplantation

A 1.5-mm diameter bone defects, in the right mandibular body below the mesial root of the lower first molar, were created in 13-week-old $ApoE^{-/-}$ and control mice as previously described [10]. $ApoE^{-/-}$ mice were then randomly assigned into group A and B and C57BL/6J mice into group C and D, with 18 mice in each group. GFP-positive BMSCs, re-suspended in α-MEM at a density of 1×10^4 cells/μl, were transplanted into group A and C via the tail vein in a total volume of 100 μl. Group B and D were injected with 100 μl α-MEM via the tail vein. Mice were sacrificed at 1, 2 and 4 weeks after surgery.

Tissue preparation and histomorphometric analysis

Following perfusion fixation with 4% paraformaldehyde the right mandibular bone was isolated. The samples were decalcified in 10% EDTA for 3 to 4 weeks and embedded in paraffin. Tissue sections, 3 μm in thickness, were cut disto-mesially. Sections selected from the most central area of the bone defects were

Table 1. Comparison of plasma lipid levels (mean ± SD, mmol/L) between ApoE-/- mice and C57BL/6J mice after 0 week and 4 weeks on a HFD

	ApoE$^{-/-}$ mice (n=10)		C57BL/6J mice (n=10)	
Plasma analytes	0 week	4 weeks	0 week	4 weeks
TG	1.13 ± 0.35	1.15 ± 0.43*	0.69 ± 0.17	0.69 ± 0.19
TC	7.08 ± 2.43	29.6 ± 4.36^{*,a}	2.25 ± 0.18	3.64 ± 0.44**
HDL	2.36 ± 0.65	4.88 ± 0.9^{*,a}	1.53 ± 0.13	2.14 ± 0.44**
LDL	1.84 ± 0.62	9.24 ± 3.03^{*,a}	0.32 ± 0.04	0.64 ± 0.24**

$^{*}p < 0.05$ vs. C57BL/6J mice (4 weeks); $^{a}p < 0.05$ vs. ApoE$^{-/-}$ mice (0 week); $^{**}p < 0.05$ vs. C57BL/6J mice (0 week).

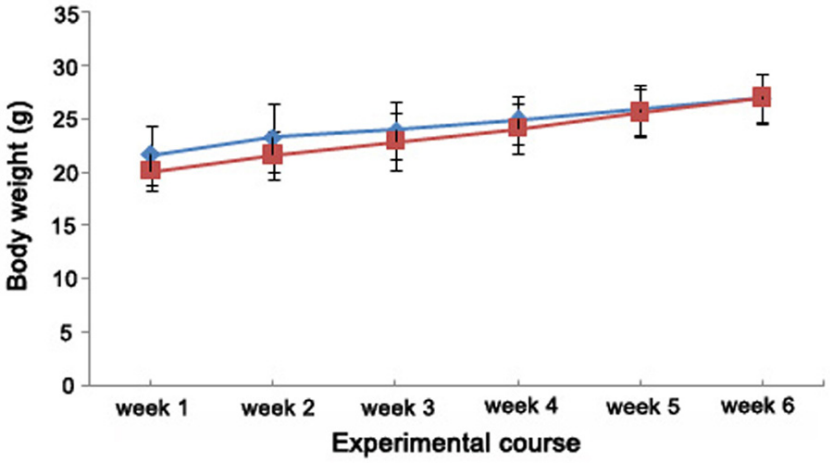

Figure 1. Comparison of body weight gain (mean ± SD, g) between C57BL/6J (n=18, diamond symbol) and ApoE$^{-/-}$ mice (n=18, square symbol) over a 6 wk period.

subjected to hematoxylin & eosin (HE) staining and Masson's Trichrome (MT) staining. Images were taken under a light microscope at ×100 magnification (Olympus, Japan) using the ProgRes CapturePro software (Jenoptik Optical Systems, Germany). For each sample, 3 HE-stained sections were selected for histomorphometric analysis using a software package (Image-Pro Plus 6.0, USA) [21]. The percentage of the newly formed bone area was defined as the ratio of new bone area to the total bone defect area.

Detection of GFP positive BMSCs

To detect cells present in the bone defect under a fluorescent microscope (Leica, Germany) the sections were stained with DAPI. GFP^{+} cells counterstained with DAPI were counted under ×400 magnification using Image J2x Software (National Institutes of Health, USA). Three randomly selected fields of view were analyzed from each representative sections/animal. The homing efficiency of transplanted BMSCs was expressed by the percentage of GFP^{+} cells counterstained with DAPI per total number of DAPI labelled cells.

Immunohistochemical staining

Purified rabbit anti-GFP polyclonal antibody (1:200; Cell signaling, USA) was used for the immunodetection of GFP. Following de-waxing and hydration, tissue sections were treated with 3% H_2O_2 for 10 min to quench endogenous peroxidase. After overnight incubation with the primary antibody at 4°C, the slides were incubated with anti-rabbit secondary antibody (ZSGB-BIO, Beijing, China). Mayer's hematoxylin was used for counter stain. Control staining was performed with normal rabbit serum without the primary antibody.

Statistical analysis

All data were expressed as mean ± SD. Statistical analysis was performed using a statistical package (SPSS 19.0, SPSS Inc, USA). Histomorphometric data were analyzed using two-way ANOVA with LSD corrections. Data of serum lipid levels and homing efficiency were analyzed using Independent-Samples T Test. Values of p lower than 0.05 were considered statistically significant.

Results

Serum lipid levels in ApoE$^{-/-}$ mice were significantly elevated after fed with HFD for four weeks

After fed with the HFD for 4 weeks, serum lipid levels were dramatically higher in ApoE$^{-/-}$ mice

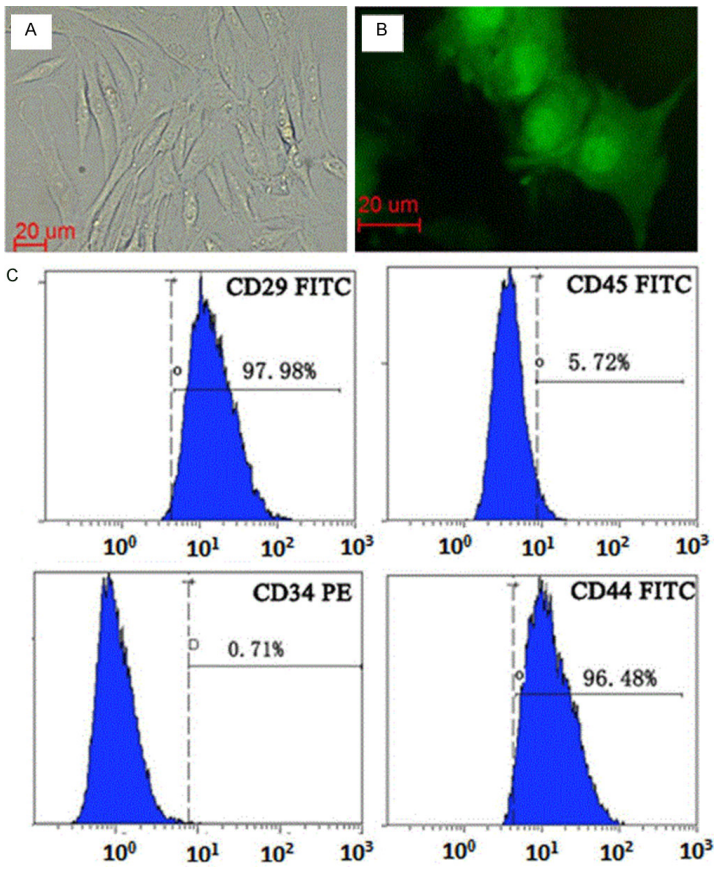

Figure 2. Characterization of BMSCs. A. In vitro culture of BMSCs. B. Expression of GFP in BMSCs cultured in vitro. C. Flow cytometry analysis showed that the 4th generation BMSCs expressed CD44 and CD29 but not CD45 or CD34. Scale bars, 20 μm.

than in C57BL/6J mice. Briefly, ApoE$^{-/-}$ mice showed an 8.1-fold increase in TC levels and a 14.4-fold increase in LDL levels when compared with the control mice. In contrast, only a 2.3-fold increase in serum HDL levels and a 1.7-fold increase in serum TG levels were detected in ApoE$^{-/-}$ mice when compared with the control (**Table 1**). These results indicated that a diet-induced hyperlipidemic model was successfully established in ApoE$^{-/-}$ mice. Body weight of both ApoE$^{-/-}$ and C57BL/6J mice increased continuously. No significant difference in body weight was detected between the two mouse strains all through the experimental period (**Figure 1**).

Characterization of BMSCs

BMSCs expressed CD44^{+} (96.48%), CD29^{+} (97.98%), CD31^{-} and CD45^{-}, which are markers for BMSCs, indicating the cultured BMSCs were of high purity. GFP could be detected 48 h post-transfection in BMSCs and expressed stably as the cell passage increased (**Figure 2**).

New bone formation was significantly inhibited in mice with hyperlipidemia

At one week post-operation, bone defects in all of the four groups were filled with abundant connective tissue containing large numbers of fibroblasts and a small amount of inflammatory cells. At two weeks after surgery, collagen fiber build-up was evident and some small islands of osteoid were also detected in the center of the bone defects. Newly formed woven bone were observed on the margins and extended towards the center of the defect. By the fourth week, all groups showed advanced bone formation and calcification. Observation of the MT-stained sections showed large area of dark blue color in all groups and reddish matured bone was identified in group C (**Figure 3A**, **3B**).

Considering the fact that none of the four groups demonstrated obvious new bone formation at one week after surgery, the newly formed bone area was only determined in bone samples isolated at 2 weeks and 4 weeks after surgery. Our results showed that at 2 weeks after surgery, the newly formed bone area in group A, B, C and D was 8.6%, 4.4%, 10.8% and 5.8% respectively. Furthermore, the differences between group A and B, group A and C, group C and D, and group B and D were all statistically significant. Similarly, at 4 weeks after surgery, the newly formed bone area was 18.6%, 13.6%, 23% and 15.7% in group A, B, C and D respectively. The differences were statistically significant (**Figure 3C**).

Homing efficiency of systemically transplanted BMSCs was compromised in mice with hyperlipidemia

The DAPI-stained slices were observed using fluorescence microscopy and GFP^{+} cells counterstained with DAPI were examined. The results demonstrated that a large number of GFP^{+} fibroblast-like cells were observed in the

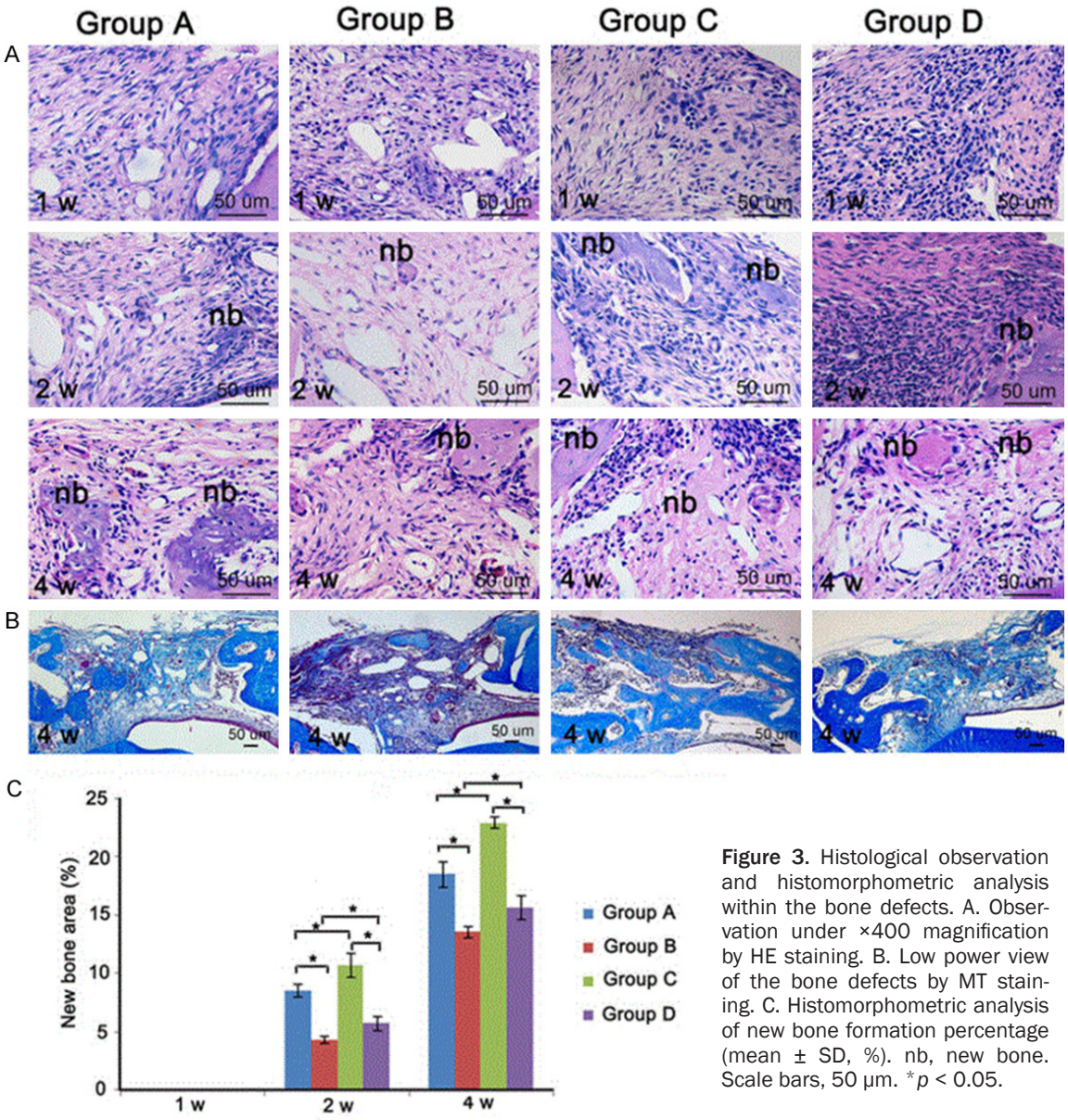

Figure 3. Histological observation and histomorphometric analysis within the bone defects. A. Observation under ×400 magnification by HE staining. B. Low power view of the bone defects by MT staining. C. Histomorphometric analysis of new bone formation percentage (mean ± SD, %). nb, new bone. Scale bars, 50 μm. $^{*}p < 0.05$.

mandibular defect 1 week and 2 weeks after transplantation. Four weeks post transplantation, the number of GFP^{+} cells decreased and some GFP^{+} osteoblasts were detected in the newly formed bone area (**Figure 4A**). Cell counting showed at the same time point, the number of GFP^{+} cells in C57BL/6J mice was significantly more than that in $ApoE^{-/-}$ mice ($p< 0.05$) (**Figure 4C**). Similar results were observed in immunohistochemical analysis. Strong expression of GFP was detected within the bone defect. In the 2nd and 4th week, GFP^{+} osteoblasts were seen in the surface and inside of newly formed bone which further indicated transplanted BMSCs can home to the mandibular defect and participate in the bone regeneration (**Figure 4B**).

Discussion

Serving as a high-affinity ligand for several lipoprotein receptors including the LDL receptor, LDL receptor-related protein, and the very low density lipoprotein receptor, the 34-kDa arginine-rich apolipoprotein E (ApoE) plays a crucial role in the regulation of lipid metabolism [22]. Since the development of $ApoE^{-/-}$ mice were reported by two independent laboratories in the 1990s [23, 24]. $ApoE^{-/-}$ mice have been a

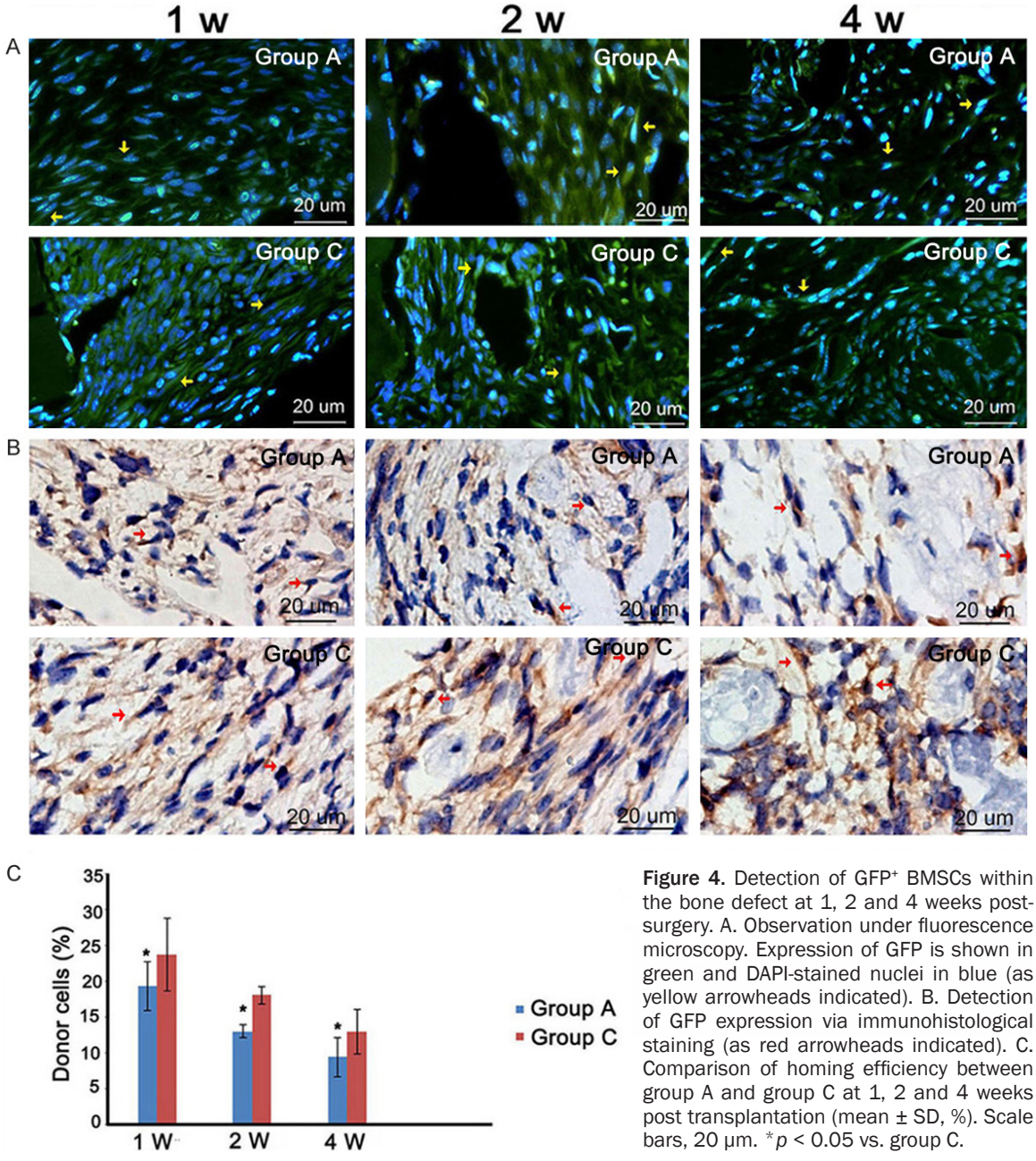

Figure 4. Detection of GFP+ BMSCs within the bone defect at 1, 2 and 4 weeks post-surgery. A. Observation under fluorescence microscopy. Expression of GFP is shown in green and DAPI-stained nuclei in blue (as yellow arrowheads indicated). B. Detection of GFP expression via immunohistological staining (as red arrowheads indicated). C. Comparison of homing efficiency between group A and group C at 1, 2 and 4 weeks post transplantation (mean ± SD, %). Scale bars, 20 μm. $^{*}p < 0.05$ vs. group C.

widespread model of severe hyperlipidemia and spontaneous atherogenesis. Feeding ApoE$^{-/-}$ mice with a HFD leads severe shift in serum cholesterol levels [25]. In the current study, hyperlipidemia was established using ApoE$^{-/-}$ mice fed with a HFD. Our results showed that after fed with a HFD for 4 weeks, ApoE$^{-/-}$ mice demonstrated dramatic increases in serum total cholesterol levels (8.1-fold) and serum LDL levels (14.4-fold) when compared with the control mice. This successfully established hyperlipidemic mouse model was then used in the following experiments to explore the effect of hyperlipidemia on homing potential of the systemically transplanted BMSCs and bone regeneration.

Bones are known for their regenerative capacity. The process of bone healing can be disturbed by many factors, such as inflammation, hormonal changes and elevated serum lipid levels. In this study, we found that the newly formed bone area in C57BL/6J mice (Group D) was significantly higher than that in ApoE$^{-/-}$ mice

(Group B) at 2 and 4 weeks after surgery, which is consistent with previous demonstrations that diet-induced hyperlipidemia is associated with a reduction in BMD and BMC [14, 15]. After BMSCs transplantation, significant increase in new bone formation was observed in both mouse strains (Group A and C), indicating the survival, recruitment and osteogenic potential of the systemically transplanted BMSCs. However, we found that the increase in newly formed bone area was lower in ApoE$^{-/-}$ mice (Group A) than that in the control mice (Group C), which further confirmed that bone regeneration was impaired and the therapeutic effects of systemically transplanted BMSCs were compromised in the presence of hyperlipidemia.

MSCs recruitment is known to be essential for successful bone injury repair [8, 20]. The mechanisms responsible for the recruitment of BMSCs to the site of bone injury have not yet been fully revealed. In the present study, the fact that the number of GFP^{+} cells in C57BL/6J mice was significantly higher than that in ApoE$^{-/-}$ mice strongly supported our hypothesis that hyperlipidemia inhibits bone regeneration by significantly disturbing the homing efficiency of the circulating BMSCs. To our knowledge, this is the first experiment to verify the inhibition of MSC homing efficiency by hyperlipidemia.

Bone defects in the oral and maxillofacial area has a huge influence on the patient's life. Hyperlipidemia is currently growing at a rapid rate throughout the world, which increases the risk of bone diseases. As we know, stem-cell based therapeutic approach has been a promising alternative for regenerative medicine. The ability of differentiating into various tissues makes BMSCs an attractive candidate for cell-based therapy to promote bone regeneration [21]. In our study, all animals survived and abundant donor BMSCs were detected within bone defects after BMSC transplantation. As early as 1 week after surgery, fluorescence microscopy and immunohistochemical analysis showed that the number of GFP positive fibroblast-like cells reached its peak and GFP positive osteoblasts were detected in the newly formed bone area at 2 and 4 weeks after surgery. More importantly, intravenous transplantation of BMSCs significantly increased new bone formation in both mouse strains, which were consistent with previous findings showing that systemically delivered BMSCs can home to the injury sites, differentiate into osteoblasts and enhance bone regeneration [8].

The enhancement of homing capacity of endogenous and transplanted stem cells is scientifically meritorious approaches for tissue regeneration and has been widely studied in regenerative medicine. Our findings showing that hyperlipidemia disturbs the homing efficiency of circulating BMSCs and inhibits new bone formation may encourage novel therapeutic approaches for hyperlipidemic patients with bone defects. Future studies should put more effort on clarifying the cellular and molecular mechanisms underlying the impaired homing capacity of BMSCs induced by hyperlipidemia.

Acknowledgements

This study was supported by Natural Science Foundation of China (No. 81271141) to PY and Natural Science Foundation of China (No. 81100757) to JZ. The authors would also like to acknowledge the grant support from central laboratory, Affiliated Hospital of Qingdao University.

Disclosure of conflict of interest

The authors declare no conflict of interest.

Address correspondence to: Dr. Pi-Shan Yang, Department of Periodontology, School of Dentistry, Shandong University, 44-1 West Wen Hua Road, Jinan, Shandong 250012. P. R. of China. Tel: +86-531-88382368; Fax: +86-531-82950194; E-mail: yangps@sdu.edu.cn; Dr. Jin Zhang, Department of Endodontics, School of Dentistry, Shandong University, 44-1 West Wen Hua Road, Jinan, Shandong 250012, P. R. of China. Tel: +86-531-88382623; Fax: +86-531-82950194; E-mail: teadenzj@sdu.edu.cn

References

[1] Schindeler A, McDonald MM, Bokko P, Little DG. Bone remodeling during fracture repair: The cellular picture. Semin Cell Dev Biol 2008; 19: 459-66

[2] Ito H. Chemokines in mesenchymal stem cell therapy for bone repair: a novel concept of recruiting mesenchymal stem cells and the possible cell sources. Mod Rheumatol 2011; 21: 113-21.

[3] Shirley D, Marsh D, Jordan G, McQuaid S, Li G. Systemic recruitment of osteoblastic cells in fracture healing. J Orthop Res 2005; 23: 1013-21.

[4] Griffin M, Iqbal SA, Bayat A. Exploring the application of mesenchymal stem cells in bone repair and regeneration. J Bone Joint Surg [Br] 2011; 93-B: 427-34.
[5] Caplan AI. Adult mesenchymal stem cells for tissue engineering versus regenerative medicine. J Cell Physiol 2007; 213: 341-7.
[6] Matziolis D, Tuischer J, Matziolis G, Kasper G, Duda G, Perka C. Osteogenic predifferentiation of human bone marrow-derived stem cells by short-term mechanical stimulation. Open Orthop J 2011; 5: 1-6.
[7] Undale AH, Westendorf JJ, Yaszemski MJ, Khosla S. Mesenchymal stem cells for bone repair and metabolic bone diseases. Mayo Clin Proc 2009; 84: 893-902.
[8] Li S, Tu Q, Zhang J, Stein G, Lian J, Yang PS, Chen J. Systemically transplanted bone marrow stromal cells contributing to bone tissue regeneration. J Cell Physiol 2008; 215: 204-9.
[9] Ponte AL, Marais E, Gallay N, Langonne A, Delorme B, Herault O, Charbord P, Domenech J. The in vitro migration capacity of human bone marrow mesenchymal stem cells: comparison of chemokine and growth factor chemotactic activities. Stem Cells 2007; 25: 1737-45.
[10] Zhang J, Tu Q, Grosschedl R, Kim MS, Griffin T, Drissi H, Yang P, Chen J. Roles of SATB2 in osteogenic differentiation and bone regeneration. Tissue Eng Part A 2011; 17: 1767-76.
[11] Hsu YH, Venners SA, Terwedow HA, Feng Y, Niu T, Li Z, Laird N, Brain JD, Cummings SR, Bouxsein ML, Rosen CJ, Xu X. Relation of body composition, fat mass, and serum lipids to osteoporotic fractures and bone mineral density in Chinese men and women. Am J Clin Nutr 2006; 83: 146-54.
[12] Orozco P. Atherogenic lipid profile and elevated lipoprotein (a) are associated with lower bone mineral density in early postmenopausal overweight women. Eur J Epidemiol 2004; 19: 1105-12.
[13] Tarakida A, Iino K, Abe K. Taniguchi R, Higuchi T, Mizunuma H, Nakaji S. Hypercholesterolemia accelerates bone loss in postmenopausal women. Climacteric 2011; 14: 105-11.
[14] Turek JJ, Watkins BA, Schoenlein IA, Allen KG, Hayek MG, Aldrich CG. Oxidized lipid depresses canine growth, immune function, and bone formation. J Nutr Biochem 2003; 14: 24-31.
[15] Parhami F, Tintut Y, Beamer WG, Gharavi N, Goodman W, Demer LL. Atherogenic high-fat diet reduces bone mineralization in mice. J Bone Miner Res 2001; 16: 182-8.
[16] Gotoh M, Mizuno K, Ono Y. Takahashi M. Fluvastatin increases bone mineral density in postmenopausal women. Fukushima J Med Sci 2011; 57: 19-27.
[17] Helin-Salmivaara A, Korhonen MJ, Lehenkari P, Junnila SY, Neuvonen PJ, Ruokoniemi P, Huupponen R. Statins and hip fracture prevention--a population based cohort study in women. PLoS One 2012; 7: 1-10.
[18] Parhami F, Jackson SM, Tintut Y, Le V, Balucan JP, Territo M, Demer LL. Atherogenic diet and minimally oxidized low density lipoprotein inhibit osteogenic and promote adipogenic differentiation of marrow stromal cells. J Bone Miner Res 1999; 14: 2067-78.
[19] Pirih F, Lu J, Ye F, Bezouglaia O, Atti E, Ascenzi MG, Tetradis S, Demer L, Aghaloo T, Tintut Y. Adverse Effects of Hyperlipidemia on Bone Regeneration and Strength. J Bone Miner Res 2012; 27: 309-18.
[20] Rojas M, Xu J, Woods CR, Mora AL, Spears W, Roman J, Brigham KL. Bone marrow-derived mesenchymal stem cells in repair of the injured lung. Am J Respir Cell Mol Biol 2005; 33: 145-52.
[21] Kim BJ, Kwon TK, Baek HS, Hwang DS, Kim CH, Chung IK, Jeong JS, Shin SH. A comparative study of the effectiveness of sinus bone grafting with recombinant human bone morphogenetic protein 2–coated tricalcium phosphate and platelet-rich fibrin–mixed tricalcium phosphate in rabbits. Oral Surg Oral Med Oral Pathol Oral Radiol 2012; 113: 583-92.
[22] Kashyap VS, Santamarina-Fojo S, Brown DR, Parrott CL, Applebaum-Bowden D, Meyn S, Talley G, Paigen B, Maeda N, Brewer HB Jr. Apolipoprotein E deficiency in mice: gene replacement and prevention of atherosclerosis using adenovirus vectors. J Clin Invest 1995; 96: 1612-20.
[23] Zhang SH, Reddick RL, Piedrahita JA, Maeda N. Spontaneous hypercholesterolemia and arterial lesions in mice lacking apolipoprotein E. Science 1992; 258: 468-71.
[24] Plump AS, Smith JD, Hayek T, Aalto-Setälä K, Walsh A, Verstuyft JG, Rubin EM, Breslow JL. Severe hypercholesterolemia and atherosclerosis in apolipoprotein E-deficient mice created by homologous recombination in ES cells. Cell 1992; 71: 343-53.
[25] Sage AP, Lu J, Atti E, Tetradis S, Ascenzi MG, Adams DJ, Demer LL, Tintut Y. Hyperlipidemia Induces Resistance to PTH Bone Anabolism in Mice via Oxidized Lipids. J Bone Miner Res 2011; 26: 1197-206.